CENTER FOR TOKAMAK TRANSIENTS SIMULATION

CTTS Overview

Stephen C. Jardin

SciDAC-4 PI Meeting

Hilton Washington DC/Rockville   July 16-18, 2019

CTTS Participants

PHYSICS TEAM

- **PPPL**: C. Clauser, N. Ferraro, I. Krebs, S. Jardin, C. Liu

- **GA**: C. Kim ,L. Lao, B. Lyons, J. McClenaghan, P. Parks

- **U. Wisc**: C. Sovinec, P. Zhu

- **Utah State U**: E. Held

- **Tech X:** E. Howell, J. King, S. Kruger

- **SBU:** R. Samulyak

- **HRS Fusion**: H. Strauss

HPC TEAM

- **RPI**: M. Shephard, S. Seol, W. Tobin

- **LBL:** N. Ding, X. Li, Y. Liu, S. Williams

- **PPPL**: J. Chen

- **SBU**: R. Samulyak

26 participants
9 institutions

Center for Tokamak Transient Simulations Outline

1. Code Descriptions

2. Forces due to Vertical Displacement Events

3. Disruption Mitigation via Impurity Injections
   3.1 Stand Alone
   3.2 via code coupling

4. Runaway Electrons interacting with MHD

5. High-Performance Computing

Center for Tokamak Transient Simulations
Outline

1. Code Descriptions

2. Forces due to Vertical Displacement Events

3. Disruption Mitigation via Impurity Injections
   3.1 Stand Alone
   3.2 via code coupling

4. Runaway Electrons interacting with MHD

5. High-Performance Computing

M3D-C¹ and NIMROD solve 3D MHD Equations in Toroidal Geometry including Impurity Radiation and Runaway Electrons

$$\partial n_i / \partial t + \nabla \bullet (n_i \mathbf{V}) = \nabla \cdot D \nabla n_i + S_n$$

$$\partial n_Z^{(j)} / \partial t + \nabla \bullet (n_Z^{(j)} \mathbf{V}) = \nabla \cdot D \nabla n_Z^{(j)} + I_Z^{(j-1)} n_Z^{(j-1)} - \left(I_Z^{(j)} + R_Z^{(j)} \right) n_Z^{(j)} + R_Z^{(j+1)} n_Z^{(j+1)} + S_Z^{(j)}$$

$$\left. \begin{array}{c} \partial \mathbf{A} / \partial t = -\mathbf{E} - \nabla \Phi \\ \nabla_\perp \bullet \dfrac{1}{R^2} \nabla \Phi = -\nabla_\perp \bullet \dfrac{1}{R^2} \mathbf{E} \\ \mathbf{B} = \nabla \times \mathbf{A} \end{array} \right\} \text{M3D-C1} \qquad \left. \begin{array}{c} \partial \mathbf{B} / \partial t = -\nabla \times \mathbf{E} \\ \nabla \bullet \mathbf{B} = 0 \end{array} \right\} \text{NIMROD}$$
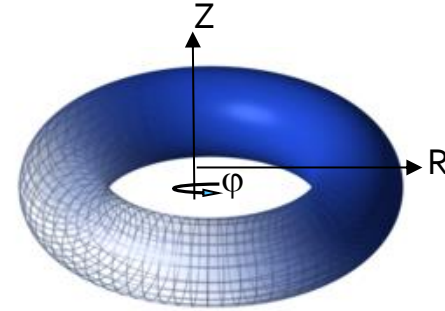
$$\rho(\partial \mathbf{V}/\partial t + \mathbf{V} \bullet \nabla \mathbf{V}) + \nabla p = \mathbf{J} \times \mathbf{B} - \nabla \bullet \mathbf{\Pi} - \varpi \mathbf{V} + \mathbf{S}_m, \qquad \mathbf{E} + \mathbf{V} \times \mathbf{B} = \eta(\mathbf{J} - \mathbf{J}_{RA}) + \mathbf{S}_{CD}$$

$$\frac{3}{2}\left[\frac{\partial p_e}{\partial t} + \nabla \bullet \left(p_e \mathbf{V} \right) \right] = -p_e \nabla \bullet \mathbf{V} + \mathbf{J} \cdot \mathbf{E} - \nabla \bullet \mathbf{q}_e + Q_\Delta + S_{eE} \qquad \mathbf{q}_{e,i} = -\kappa_{e,i} \nabla T_{e,i} - \kappa_{\|e,i} \nabla_\| T_{e,i}$$

$$\frac{3}{2}\left[\frac{\partial p_i}{\partial t} + \nabla \bullet \left(p_i \mathbf{V} \right) \right] = -p_i \nabla \bullet \mathbf{V} - \mathbf{\Pi}_i : \nabla \mathbf{V} - \nabla \bullet \mathbf{q}_i - Q_\Delta + \tfrac{1}{2}\varpi V^2 + S_{iE}$$

- Also, separate equations for resistive wall and vacuum regions
- Different options for Runaway Electron current $\mathbf{J}_{RA}$
- Option for energetic ion species (not used here)

M3D-C¹ and NIMROD have very different numerical implementations

	M3D-C¹	**NIMROD**
Poloidal Direction	Tri. C^1 Reduced Quintic FE	High. Order quad C^0 FE
Toroidal Direction	Hermite Cubic C^1 FE	Spectral
Magnetic Field	$\mathbf{B} = \nabla\psi \times \nabla\varphi - \nabla_{\perp}f' + F\nabla\varphi$	$\mathbf{B} = B_r\widehat{R} + B_z\hat{Z} + B_{\varphi}\widehat{\varphi}$
Velocity Field	$\mathbf{V} = R^2\nabla U \times \nabla\varphi + \omega R^2\nabla\varphi + R^{-2}\nabla_{\perp}\chi$	$\mathbf{V} = V_r\widehat{R} + V_z\hat{Z} + V_{\varphi}\widehat{\varphi}$
Coupling to Conductors	same matrix	Separate matrices w interface

Both codes use:
- Split Implicit Time advance
- Block-Jacobi preconditioner based on SuperLU_DIST
- GMRES based iterative solvers
- Impurity ionization and recombination rates from KPRAD

Center for Tokamak Transient Simulations
Outline

1. Code Descriptions

2. Forces due to Vertical Displacement Events

3. Disruption Mitigation via Impurity Injections
   3.1 Stand Alone
   3.2 via code coupling

4. Runaway Electrons interacting with MHD

5. High-Performance Computing

Vertical Displacement Events: (VDEs)

- Initial emphasis was to perform benchmark calculations in both 2D and 3D for code verification and validation ... also with JOREK (EU code)

- We are also validating results with data from the JET experiment

- Primary application is to ITER
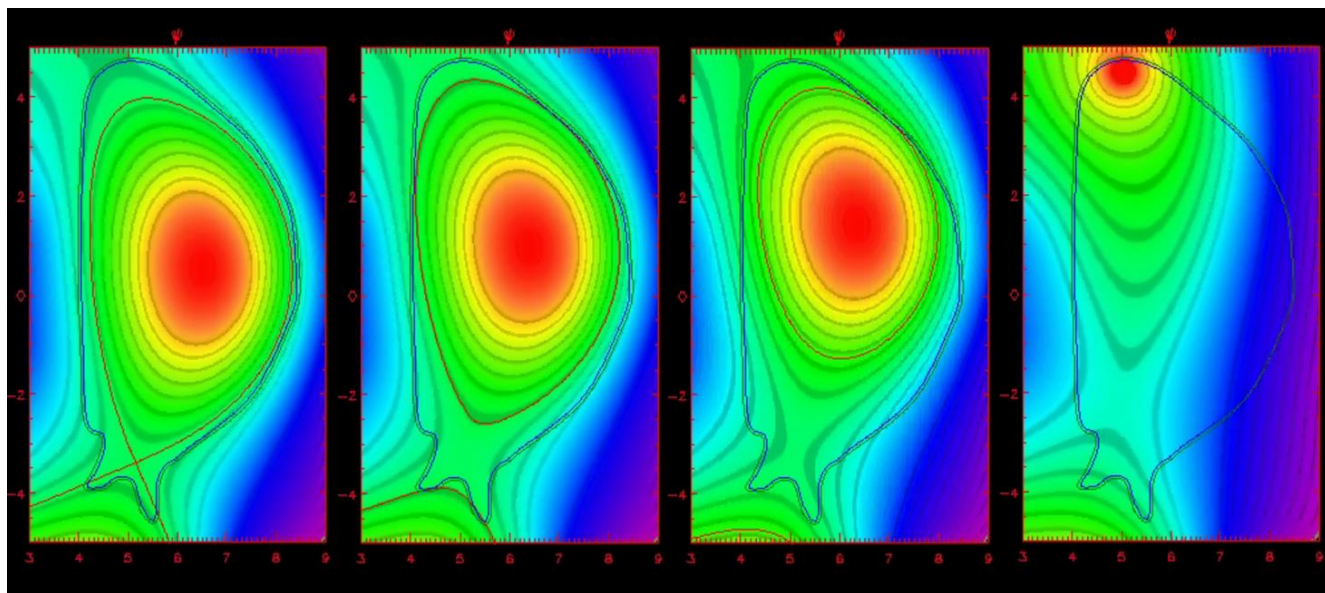
| Equilibrium | Wall contact | Start TQ | Final |

VDE can occur when position control system fails, causing discharge to move up or down and contact wall

5.3 T 15MA ITER

Linear VDE benchmark between M3D-C¹, NIMROD & JOREK

Equilibrium poloidal magnetic flux in M3D-C¹

Resistive wall

Plasma region

Vacuum region

Computational boundary

Coils

Growth Rate (s^{-1})

linear relation
JOREK (2D nonlinear)
M3D-C¹ (linear, ΔZ_{axis}=0.5mm)
M3D-C¹ (2D nonlinear)

Wall resistivity (Ω m)
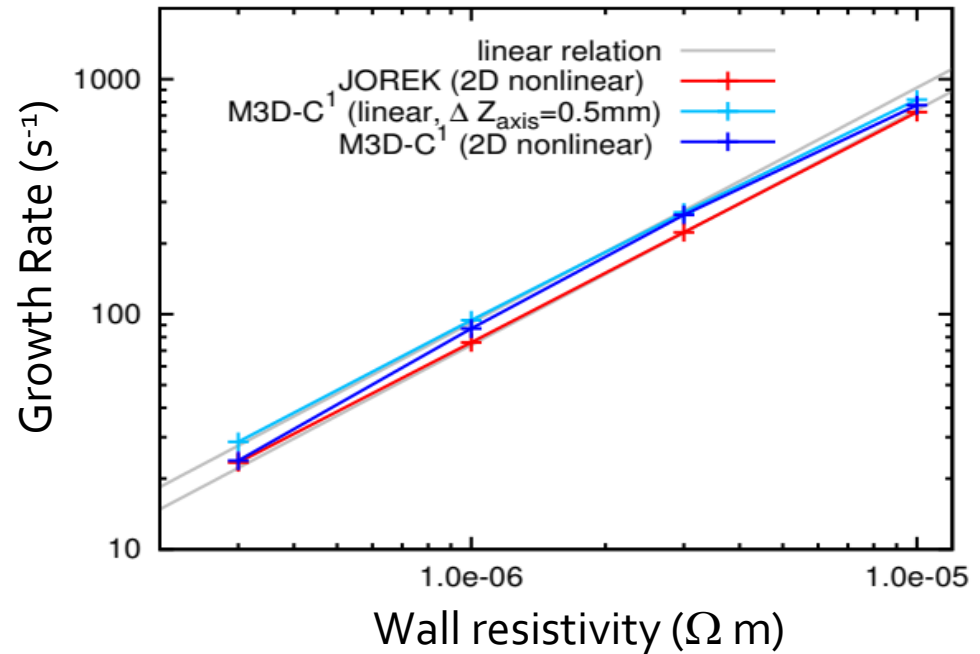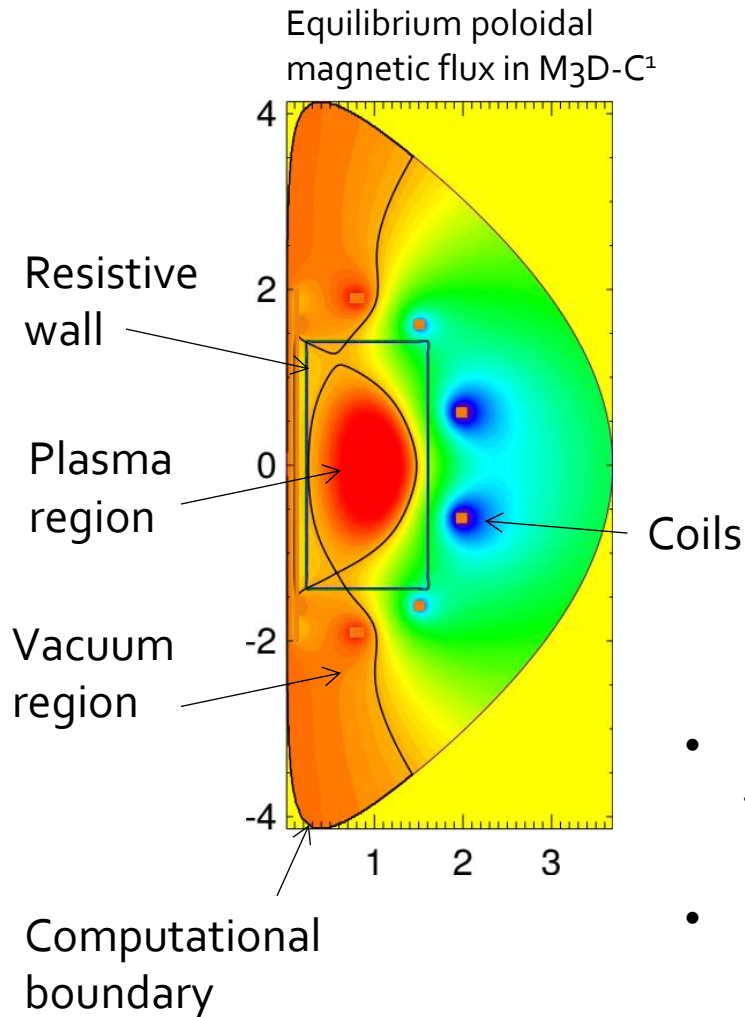
- Realistic equilibrium (NSTX) but simplified geometry that all codes can handle (rectangular resistive wall)

- Codes agree to within 20% on growth rates over wide range of wall resistivity

I. Krebs, C. Sovinec, F. Artola

9

2D <u>Nonlinear</u> VDE benchmark between M3D-C¹, NIMROD & JOREK

Poloidal magnetic flux
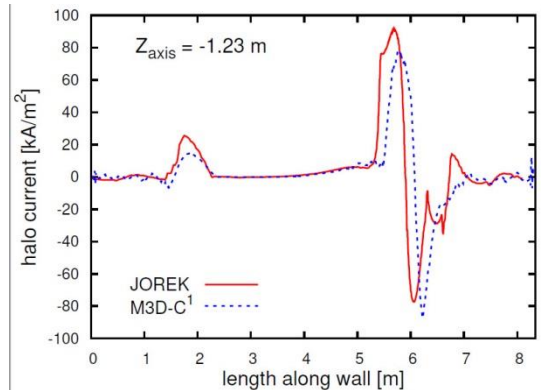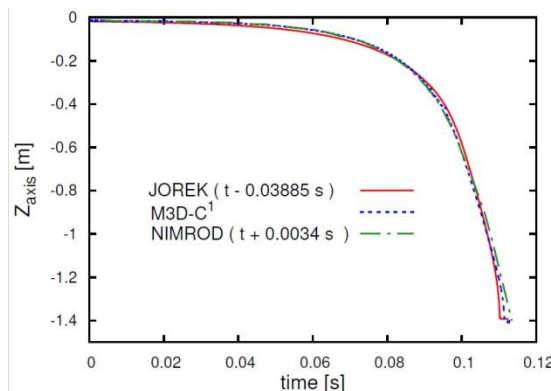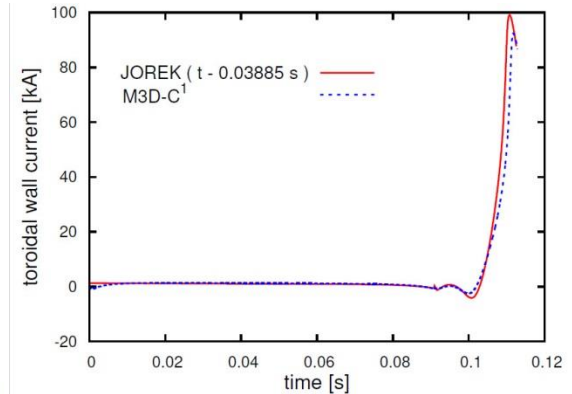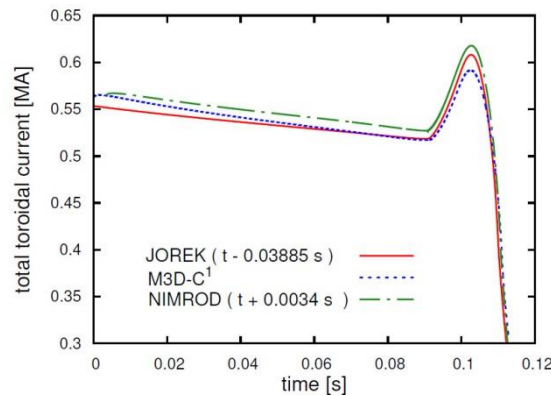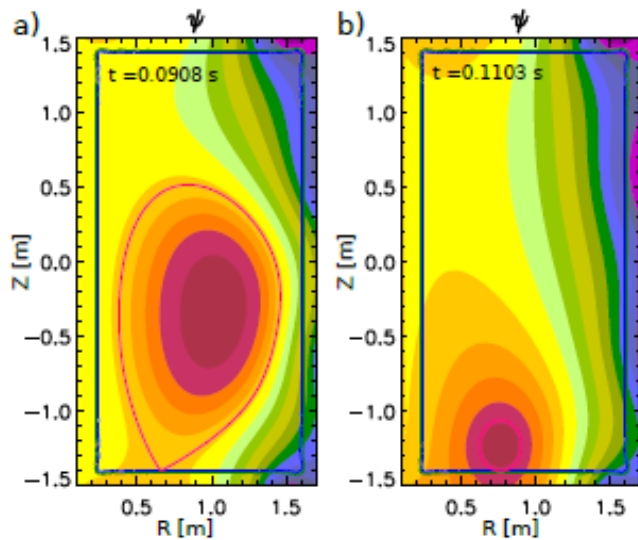
- Good agreement amongst 3 codes on time evolution plasma position, plasma and wall currents, and forces.
- Benchmark still underway to resolve small differences
- 3D benchmark to begin soon

I. Krebs, C. Sovinec, F. Artola

3D M3D-C¹ simulation of JET VDE shows origin and magnitude of sideways force – 1

Jφ

Jφ

t = 0.0 ms

t = 2.2 ms
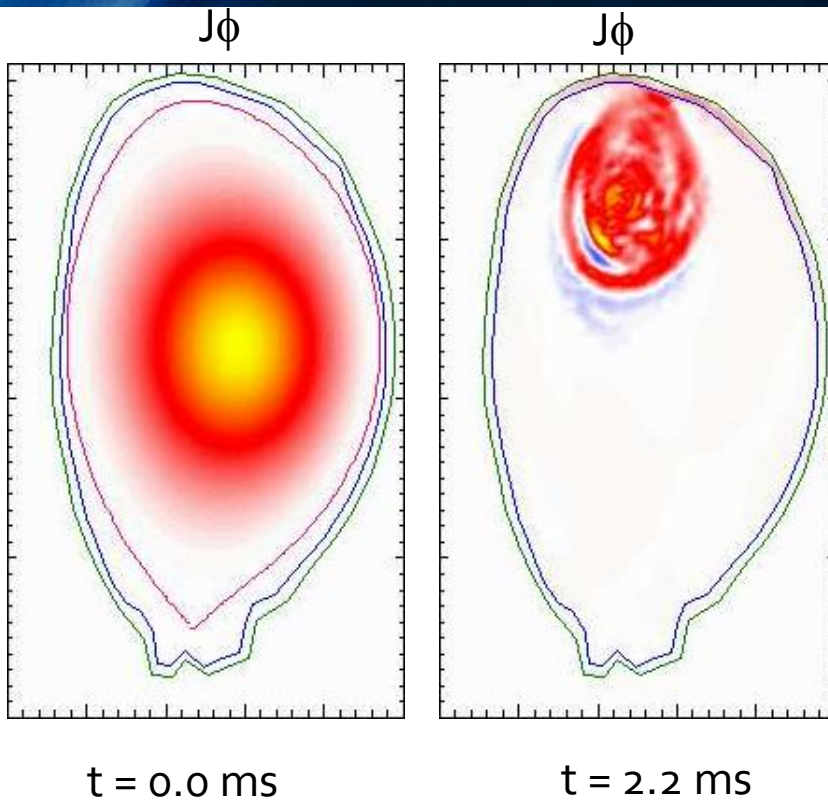
- Plasma drifts upward and scrapes off

- Sideways force arises when q(a) < 1 and large (1,1) mode develops

Legend:
- t = 0.74 ms (black)
- t = 1.14 ms (green)
- t = 1.55 ms (blue)
- t = 1.88 ms (magenta)
- t = 2.20 ms (red)

Normalized Poloidal Flux ψ

H. Strauss   11

- ΔF_{xC1} – sideways force as computed by M3D-C¹
- ΔF_{NC1} – "Noll Force" approximation from M3D-C¹
- $\Delta F_{N\,all}$ – "Noll Force" from all JET disruptions in 2011-16 ILW database
- $\Delta F_{N\,VDE}$ – "Noll Force" from JET VDE disruptions

- JET uses an approximation to the actual force called the "Noll Force"
- M3D-C¹ gives value for Noll Force mostly within 20% of experimental data using scaled values of τ_{wall}
- These are now being extended to use actual τ_{wall}

$\Delta F_X, \Delta F_N, \quad vs. \tau_{CQ}/\tau_{wall}$

Force (MN)

τ_{CQ} / τ_{wall}
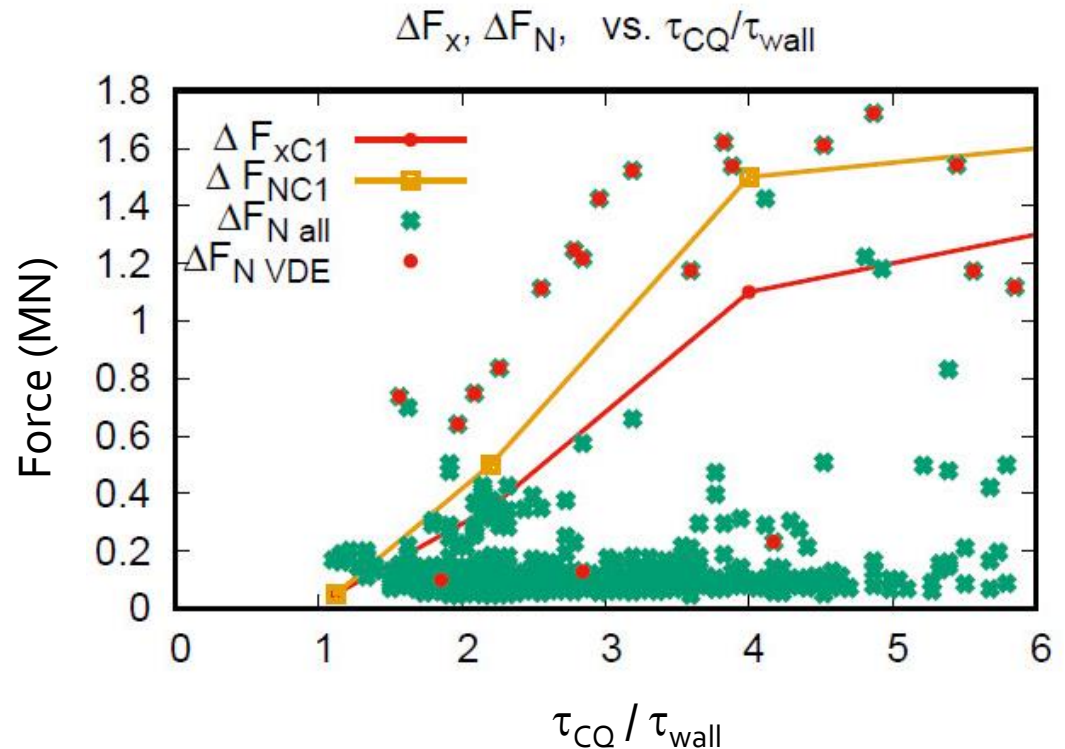
"Noll Force": $\Delta F_N = \pi B \Delta M_{IZ}$

H. Strauss

High Resolution Poloidal unstructured mesh used in ITER calculation

Full Mesh

Close-up of Plasma Region
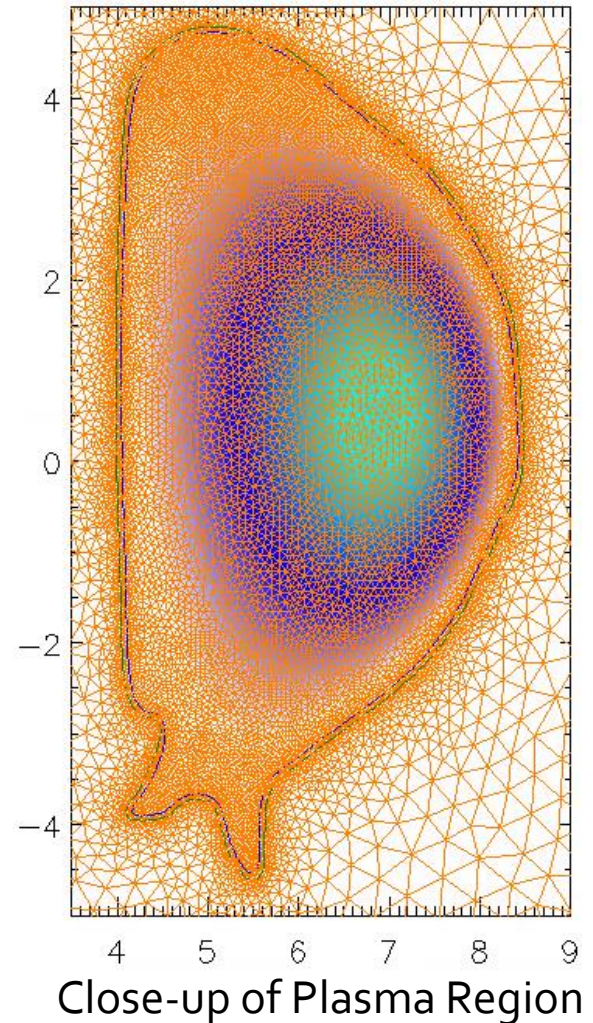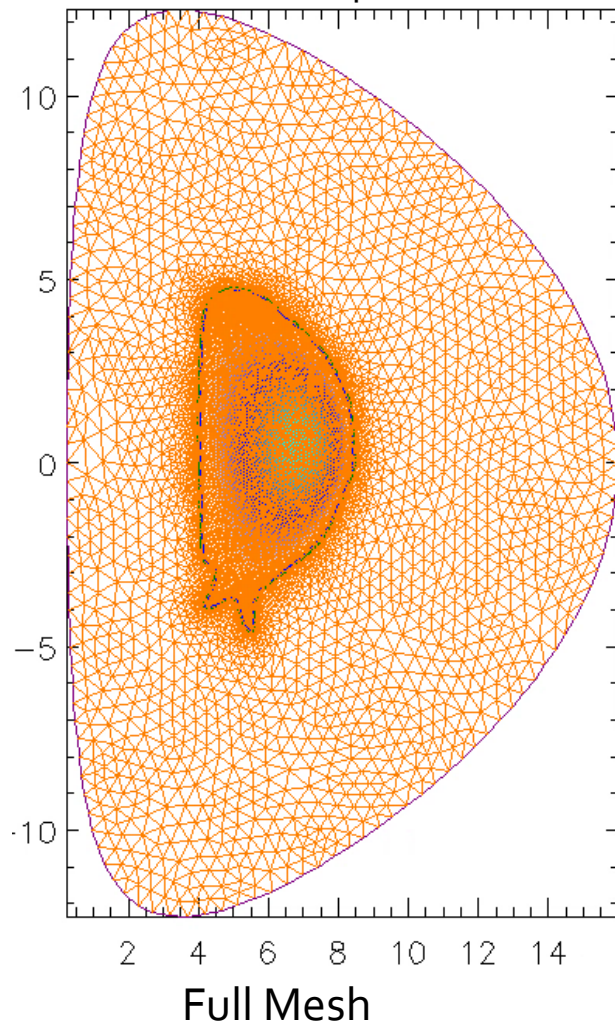
L/R time of vessel determined from simulation without plasma
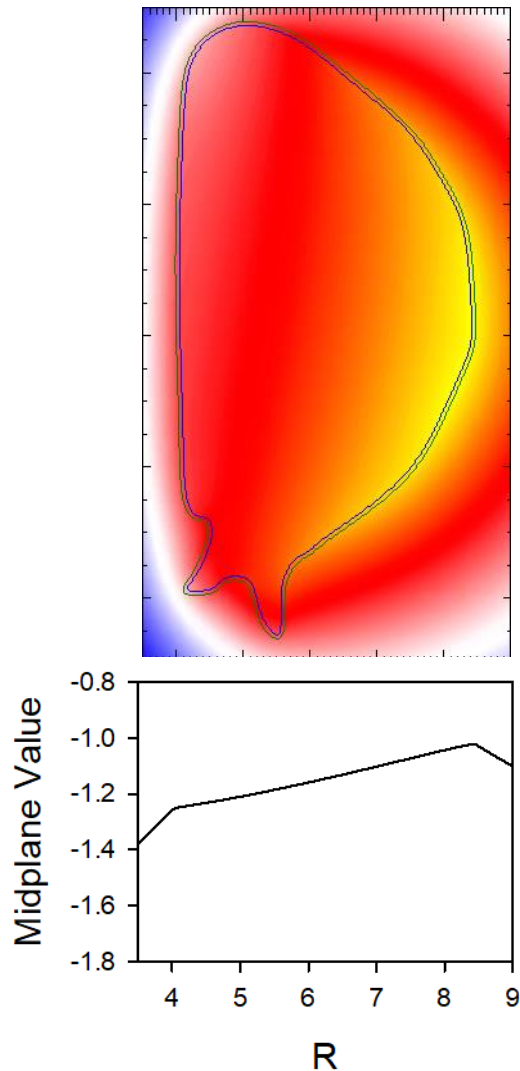
- Simulation with constant loop voltage applied at t=0 & no plasma

- Wall resistivity adjusted to give correct L/R time

FIT: $I(t) = I_0*(1. - e^{-t/T})$

T = 235 ms
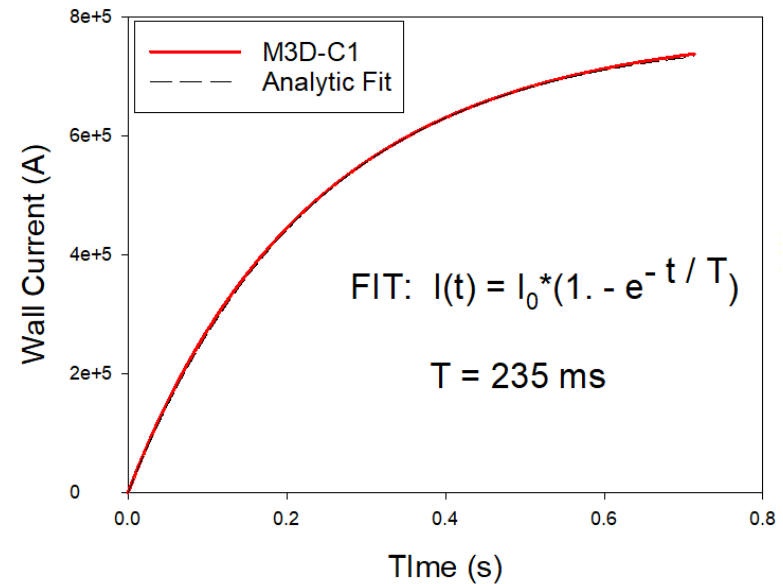
Simulation time: 1,100,000 τ_A

M3D-C¹ is being interfaced with the CARRIDI engineering code to produce realistic forces for ITER
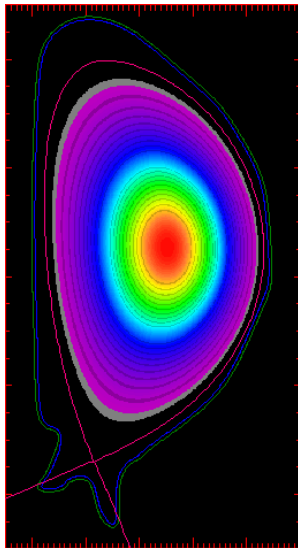
P: t = 0   P: t = 664 ms
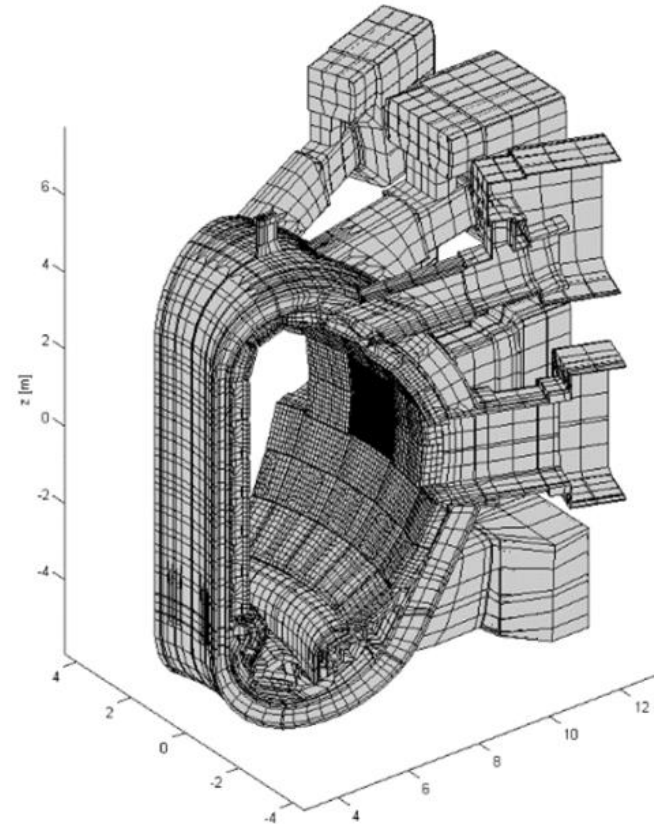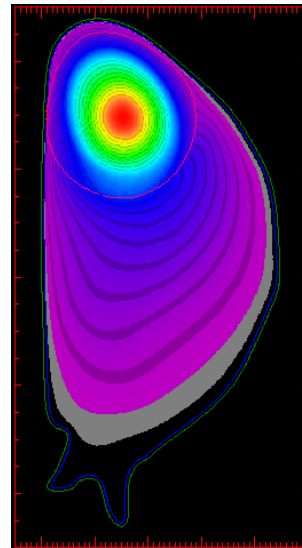
- CARRIDI is presently interfaced with the 2D equilibrium evolution code CARMA0NL

- Benchmark between M3D-C¹ & CARMA0NL was presented at EPS meeting last week

- Now interfacing M3D-C¹ VDE simulation with CARRIDI to extend analysis to 3D plasma

CARRIDI detailed electro-magnetic model of ITER structure.

C. Clauser, F. Villone

Large poloidal currents shared between plasma and structure (halo currents) develop during VDE in ITER
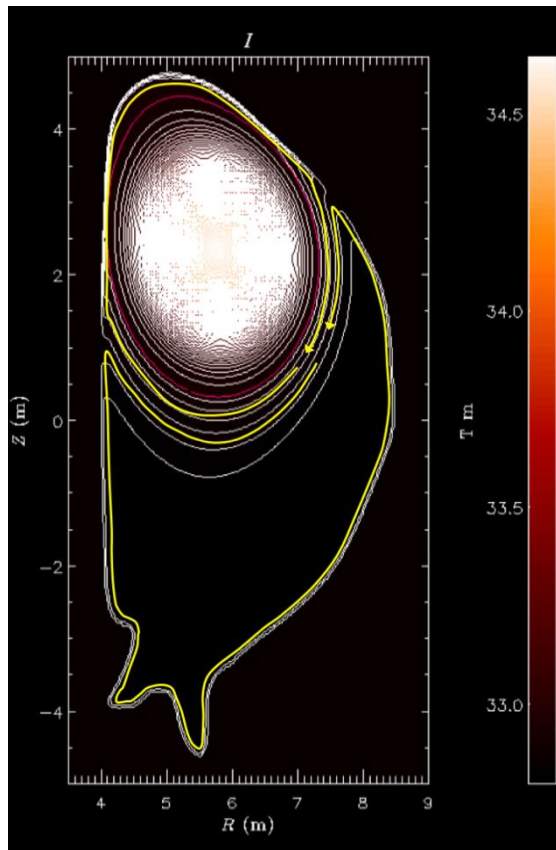
Halo currents (shown in yellow) pass between plasma and structure
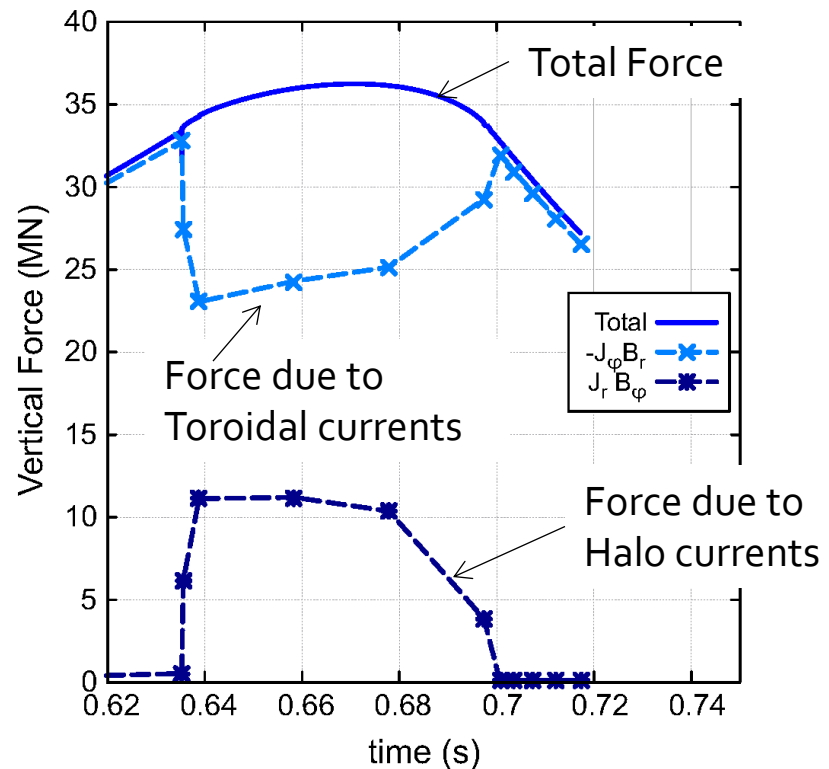
- Large force due to halo currents is compensated by reduced force due to toroidal currents !!
- However, these halo currents can produce large localized forces … evaluated with CARRIDI model

Plasma contact with surfaces during VDE leads to "sheaths" that influence disruptive dynamics.

Mag. sheath sketch from P. C. Stangeby, *Pl. Bdry. of Mag. Fus. Devices* (Taylor & Fr., 2000).

- Preferential loss of electrons induces electrostatic sheath layers.

- Magnetic field direction further influences the of outward flows.

- New sheath-based velocity boundary conditions investigated by PhD student, applied to NIMROD

  - $V_B = \sqrt{\dfrac{T_e}{m_i}} \, \widehat{b}$

- Can have significant influence on plasma evolution during VDE as shown in temperature contours in figure
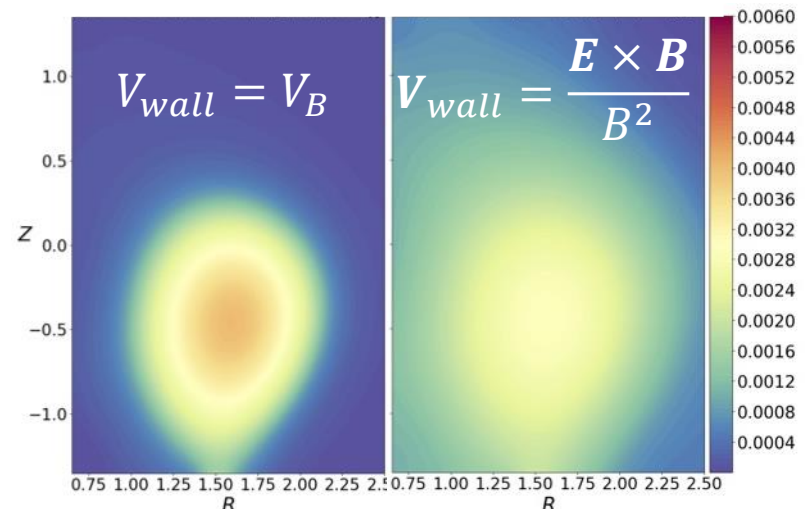
T_e profiles for computed VDEs indicate the influence of boundary conditions.

C. Bunkers, C. Sovinec

Center for Tokamak Transient Simulations Outline

M3D-C¹ & NIMROD Impurity-MHD Models Successfully Benchmarked[1]

- 2D, NL benchmark completed[1]
  - DIII-D plasma
  - Neon or argon injected on-axis

- Excellent agreement deep into nonlinear phase
  - Global quantities: P_{rad}, etc
  - Contours of T_e and J

- 3D, nonlinear benchmark in progress

Temperature

Plasma Current
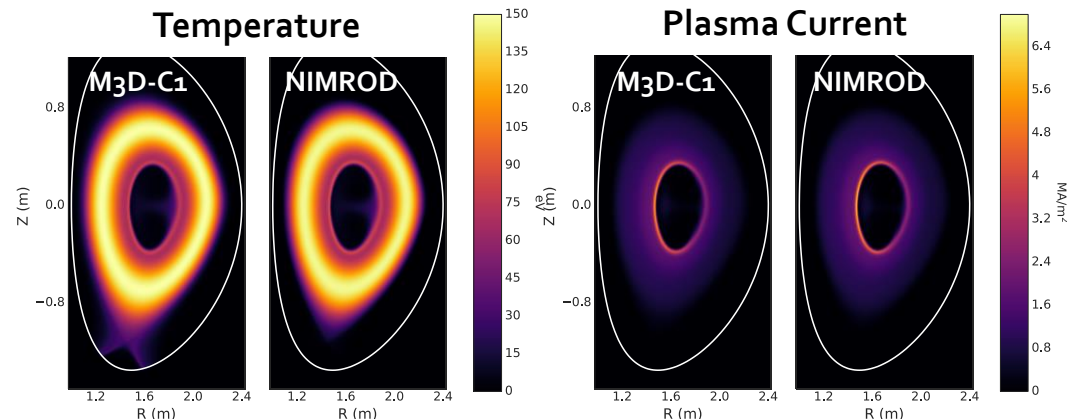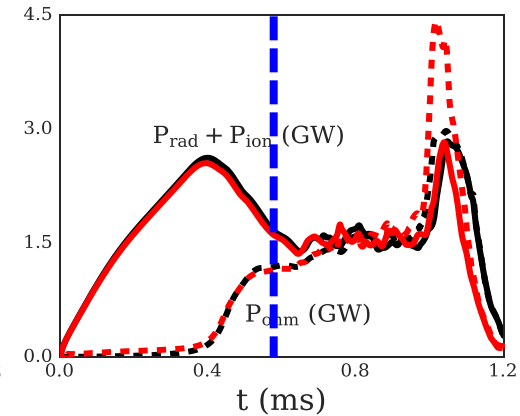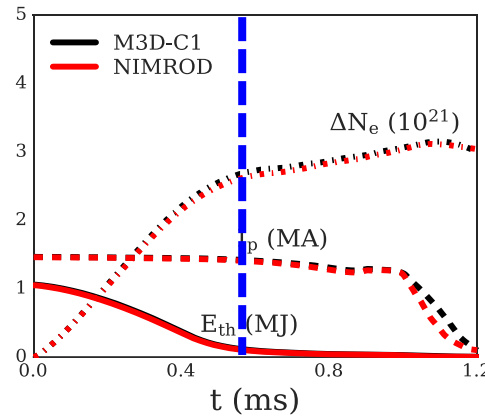
[1]B.C. Lyons et al. Plasma Phys. Control. Fusion 61, 064001 (2019).

B. Lyons, C. Kim

Electromagnetic pellet injector offers advantages for ITER; proposal to test on NSTX-U
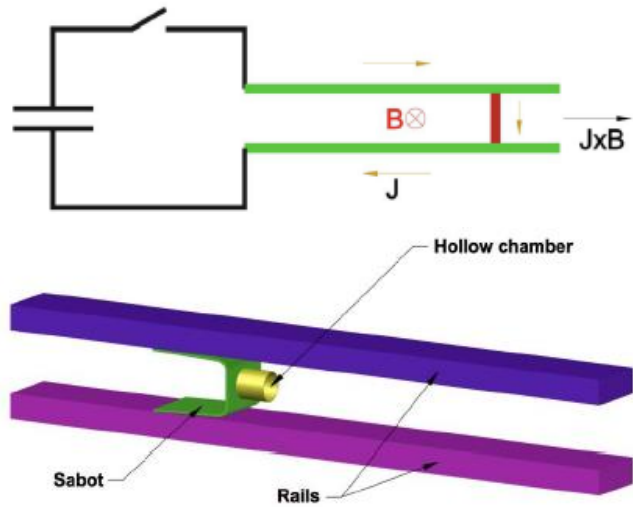
- Very fast response time (2-3 ms)

- Speeds up to 1 km/s

- High resolution modeling of 1 mm Carbon pellet as 2.5 cm (poloidal) x 12.5 cm (toroidal) Gaussian source

Electron Temperature
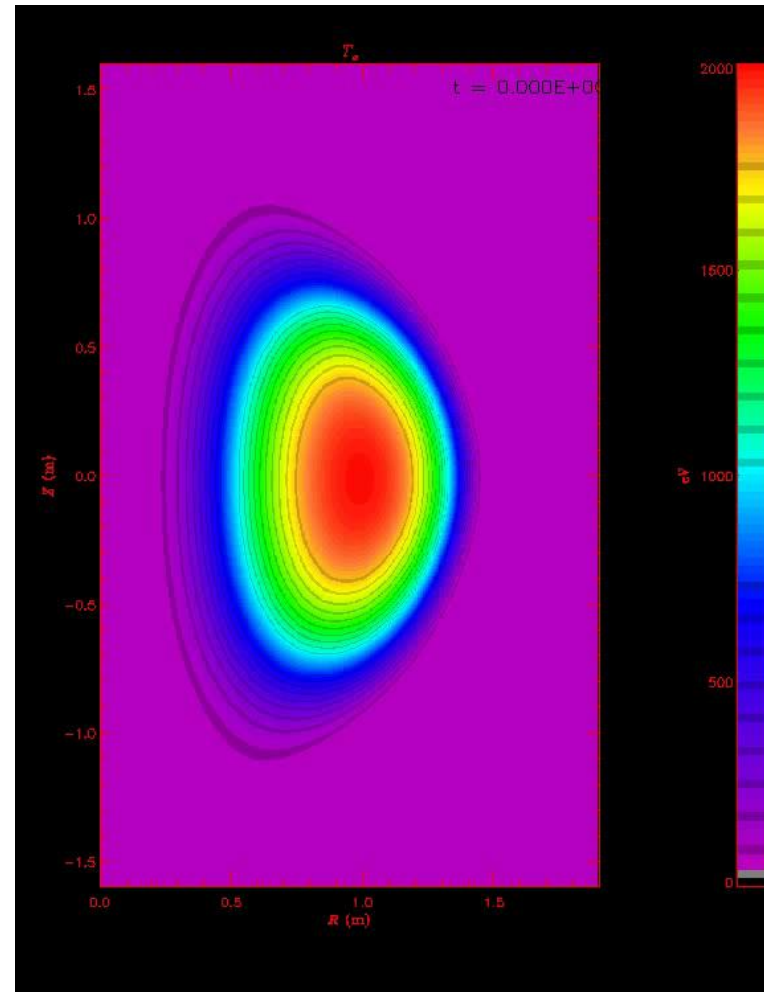
$Te(0) = 2$ keV

$n(0) = 2 \times 10^{19}$ m

$I_P = 600$ kA

$\beta p = 0.73$

$li(3) = 0.6$

4 time slices in a M3D-C¹ simulation of a 1 mm Carbon pellet injected into NSTX-U via EPI

Injection Plane Contours at different times

	(a) 0.065 ms	(b) 0.324 ms	(c) 0.648 ms	(d) 0.973 ms

Change in Electron Temp.

(a) - 0.6 keV
(b) - 1.7 keV
(c) - 1.7 keV
(d) -1.7 keV

Carbon Density:

(a) 6.8×10^{19} m^{-3}
(b) 5.2×10^{19} m^{-3}
(c) 5.2×10^{19} m^{-3}
(d) 3.1×10^{19} m^{-3}

Radiation source:

(a) - 3.2. GW/m^3
(b) - 1.0 GW/m^3
(c) - 1.1 GW/m^3
(d) - 0.4 GW/m^3
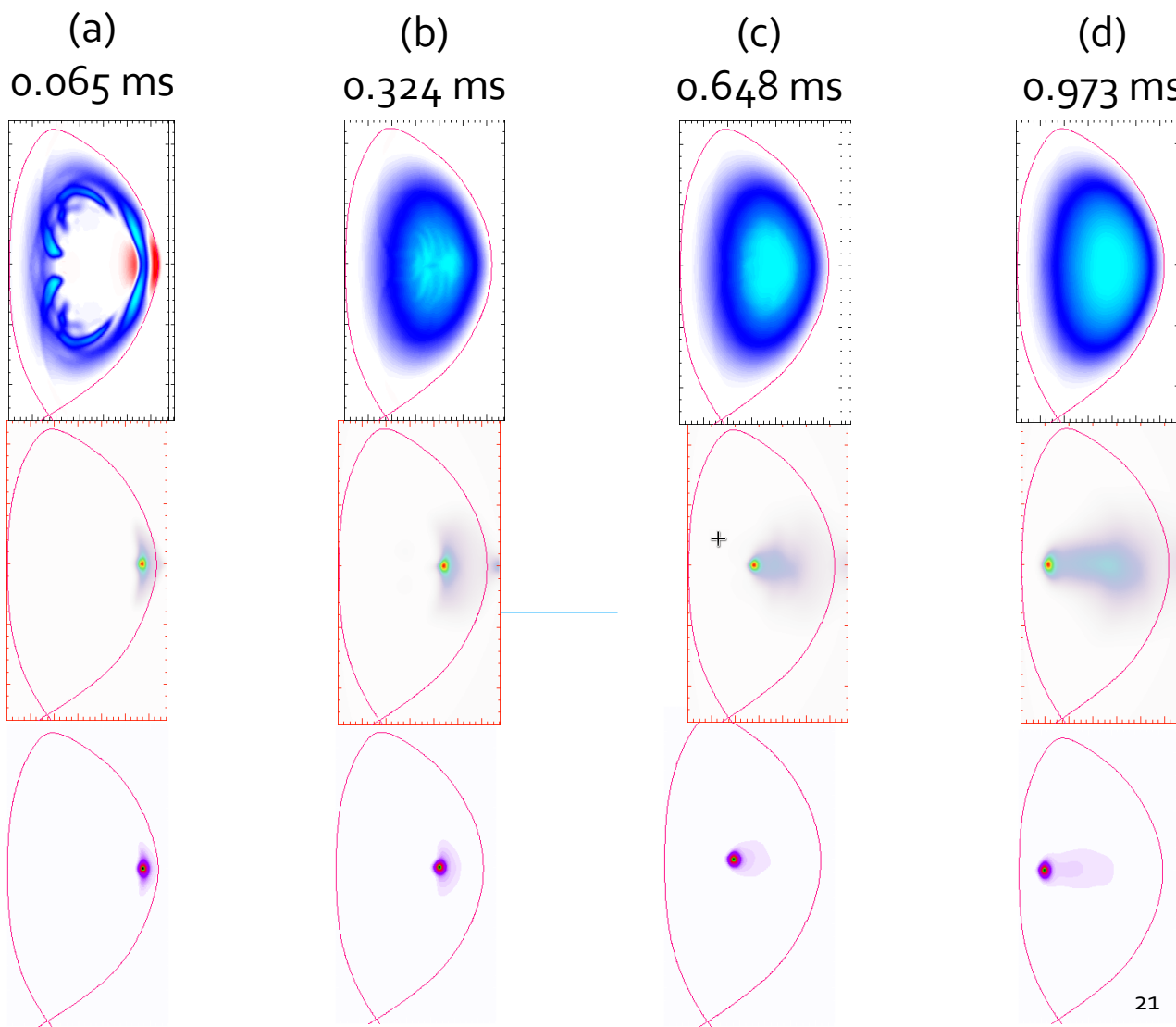
Same time (t=0.130 ms), different toroidal locations

| (a) $\varphi = 0^{\circ}$ | (b) $\varphi = 90^{\circ}$ | (c) $\varphi = 180^{\circ}$ | (d) $\varphi = 270^{\circ}$ |

Change in Electron Temp.

(a) – 969. eV
(b) - 1062 eV
(c) – 1034 eV
(d) - 1067eV

Carbon Density:

(a) 8.20×10^{19} m^{-3}
(b) 1.86×10^{19} m^{-3}
(c) 0.07×10^{19} m^{-3}
(d) 1.86×10^{19} m^{-3}

Radiation source:

(a) - 4400 MW/m^3
(b) - 40. MW/m^3
(c) - 0.5 MW/m^3
(d) -40. MW/m^3
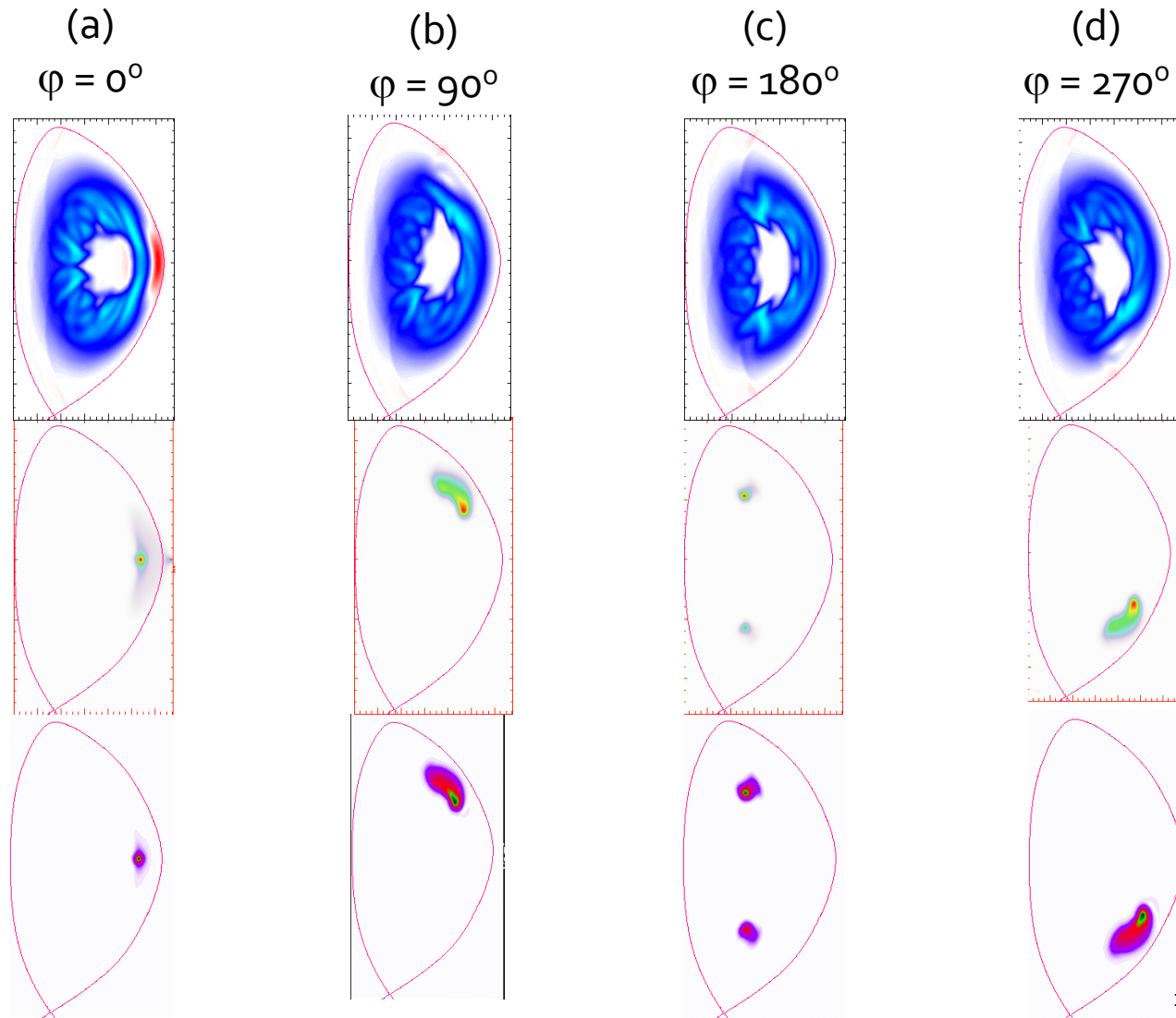
Comparison of Dual SPI injector on DIII-D with Single injector…same total impurity

Magnetic Energy n=[1,2,3,4] Single Injector

Magnetic Energy n=[1,2,3,4] Dual Injector
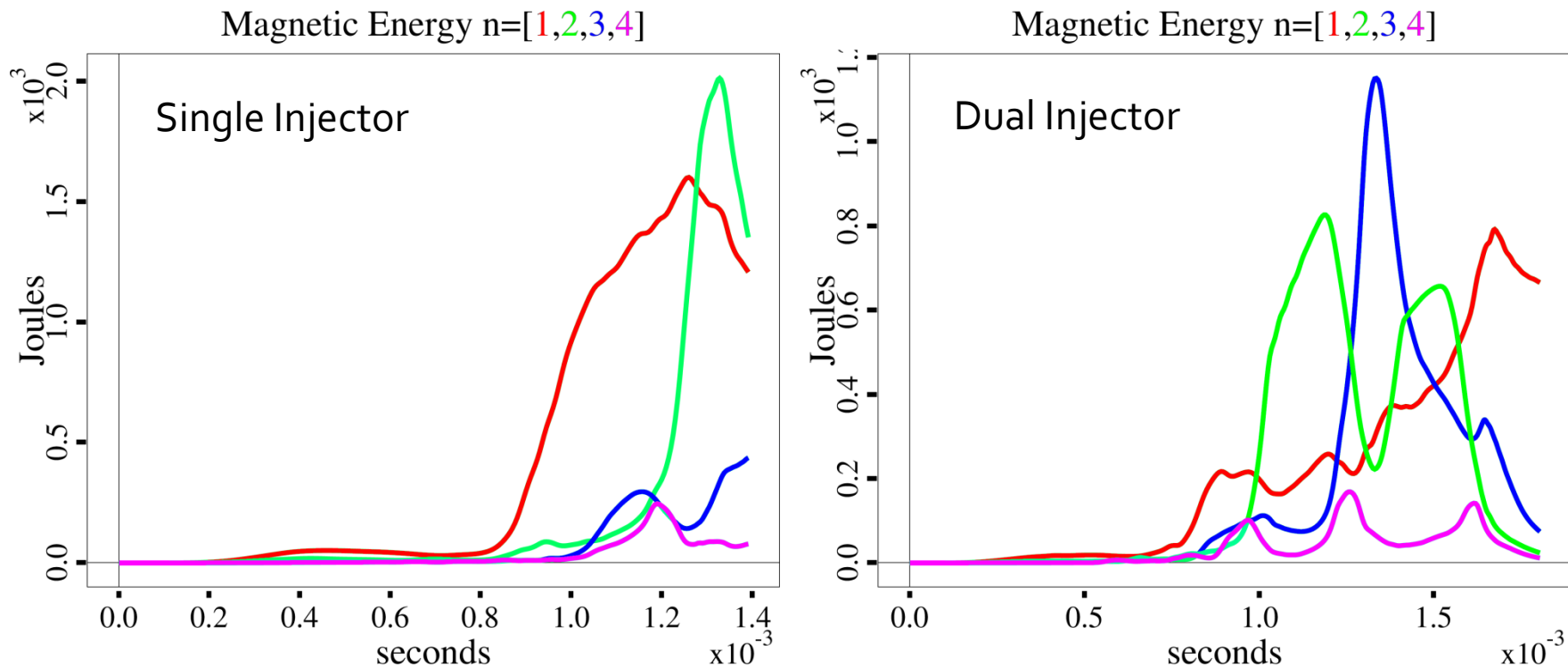
Dual injector (on right, separated by 120°) shows less energy in low-n MHD modes, which leads to a more benign thermal quench

NIMROD simulation

C. Kim

Animation of dual injection showing Impurity Density and Radiation contours
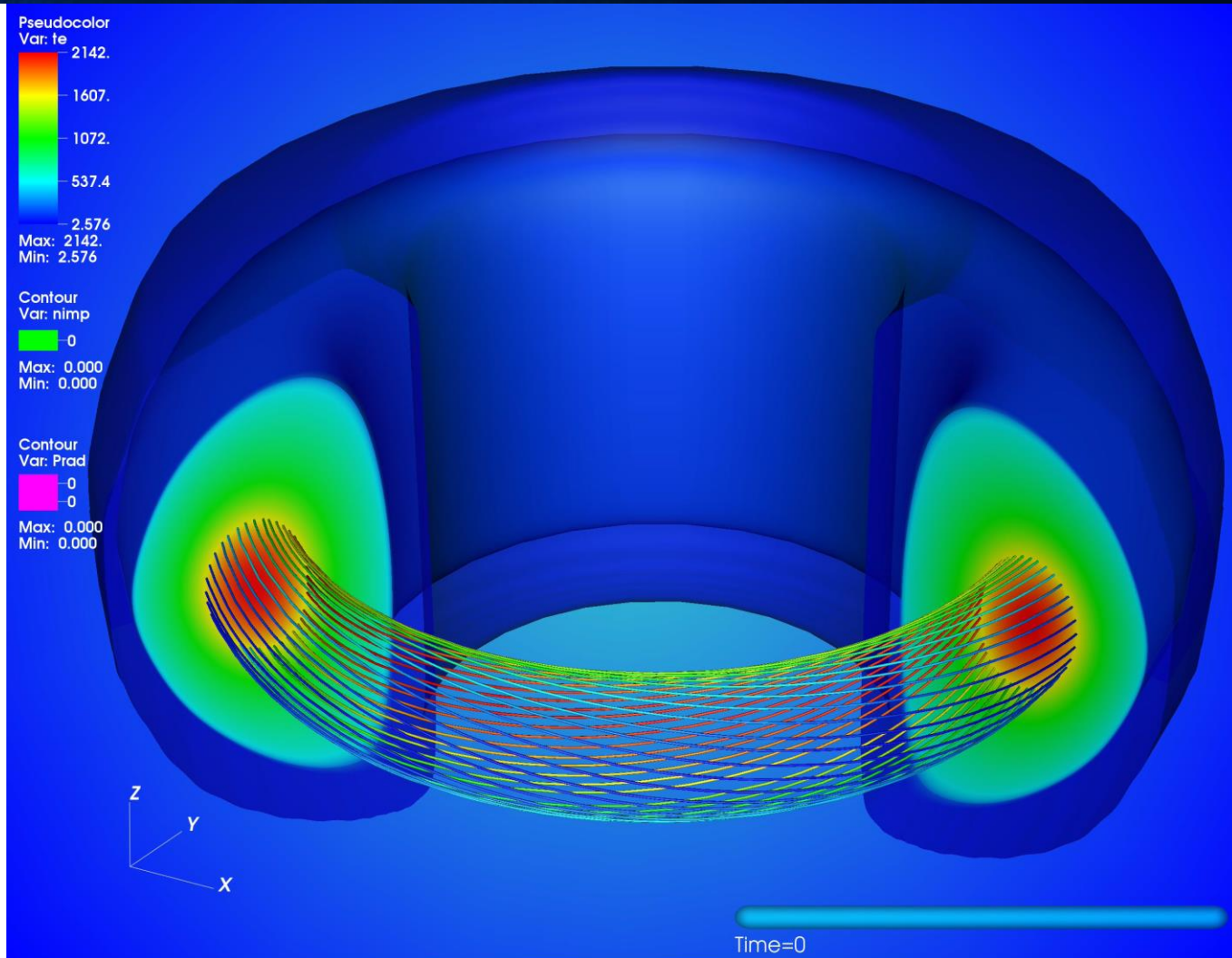
C. Kim

Center for Tokamak Transient Simulations
Outline

1. Code Descriptions

2. Forces due to Vertical Displacement Events

3. Disruption Mitigation via Impurity Injections
   3.1 Stand Alone
   3.2 via code coupling

4. Runaway Electrons interacting with MHD

5. High-Performance Computing

Accurate Modeling of Disruption Mitigation by Shattered Pellet Injection (SPI) Requires Coupling of Local Pellet Models to Global 3D Extended MHD Codes

- A multi-scale problem with spatial scales ranging from millimeters to 10x meters

- A two-level approach is adopted.

LOCAL MODEL
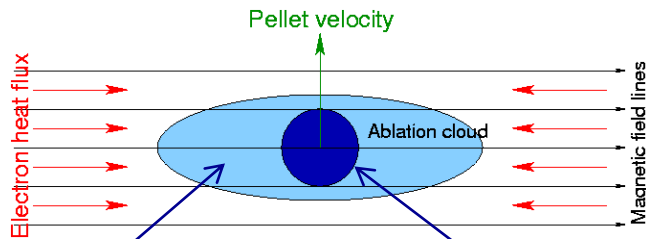
- Ablation of SPI fragments in tokamaks

- Kinetic model for the electron-heating of ablated gas
- Low magnetic Re MHD equations
- EOS with atomic processes
- Radiation and Conductivity models
- Pellet cloud charging models
- ∇B drift models for ablated material

GLOBAL MODEL
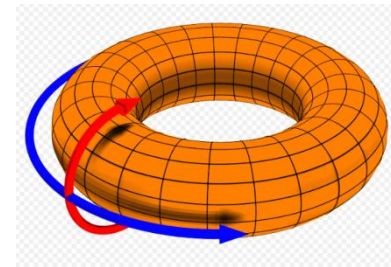
- NIMROD, M3D-C[1]
  - Fluid equations for density, momentum, and temperature
  - Magnetic Field Evolution
  - Continuity eqs. for each charge state
  - Coupled by ionization/recombination
  - Calculates radiated power

For the Local Pellet Physics Model Two Codes with Different Numerical Schemes Are Used

Their agreement with certain classes of problems is important for our V&V program.

FronTier

- Hybrid Lagrangian-Eulerian code with explicit interface tracking
- Both pellet surface and ablation cloud – plasma interface are explicitly tracked
- 2D axisymmetric simulation of the ablation of single neon pellet.
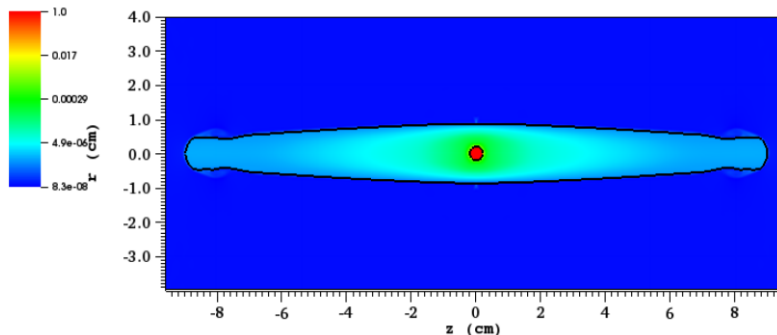
Lagrangian Particle code (LP)

- Highly adaptive 3D code
- Lagrangian treatment of ablation material eliminates numerous numerical difficulties associated with ambient plasma, fast time scales etc.
- Simulate SPI fragments in 3D
- Used for coupling with NIMROD and M3D-C[1]

R. Samulyak

27
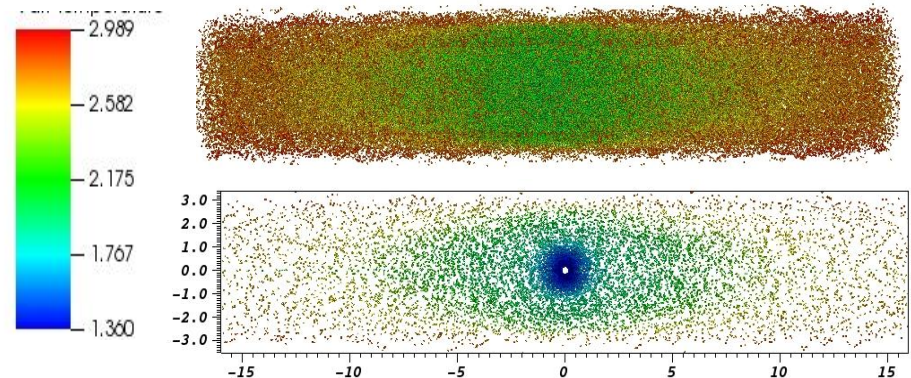
Both Local Codes Have Successfully Passed a Set of Verification Tests

- Both codes compared to theory in spherical symmetry
- Good agreement with scaling laws
- Computation of pellet ablation database is underway (dependence on B and plasma parameters)

- 3D LP was used to compute parallel expansion of ablated cloud up to 10 m. Excellent agreement with legacy 1D code.

- Reduction of the ablation rate in magnetic fields due to longer and narrower channels
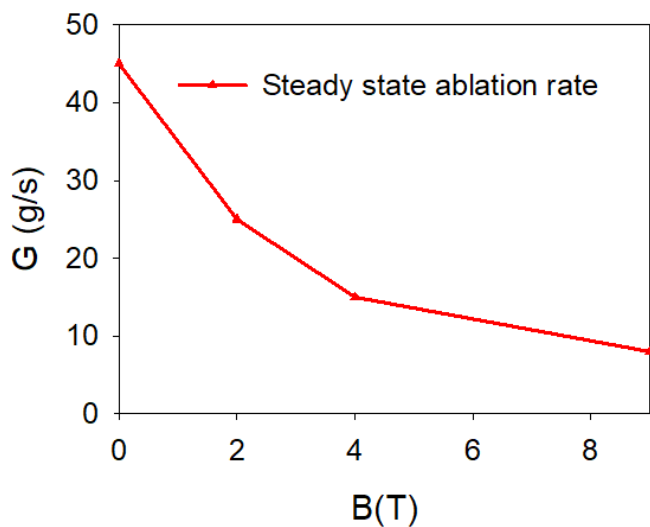
Comparison of theory and simulations of ablation rate and states at the sonic radius

	G(g/s)	r* (cm)	P* (bar)	T* (ev)
Theory	64.44	0.595	6.104	6.19
Simulation	63.77	0.593	6.096	6.21

Interacting flows in LP simulation of SPI fragments

R. Samulyak
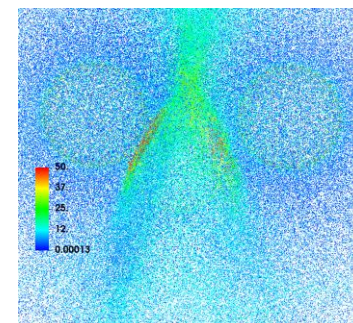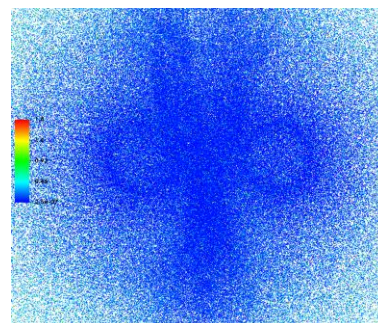
An Iteration Algorithm Has Been Developed to Test Multi-Scale Coupling of LP to Global NIMROD / M3D-C^1 MHD Codes

NIMROD simulation domain showing ablated material obtained from LP code

LP simulation of pellet ablation cloud

B, n_e, T_e from TK to LP

∇ B - drifted ablation material
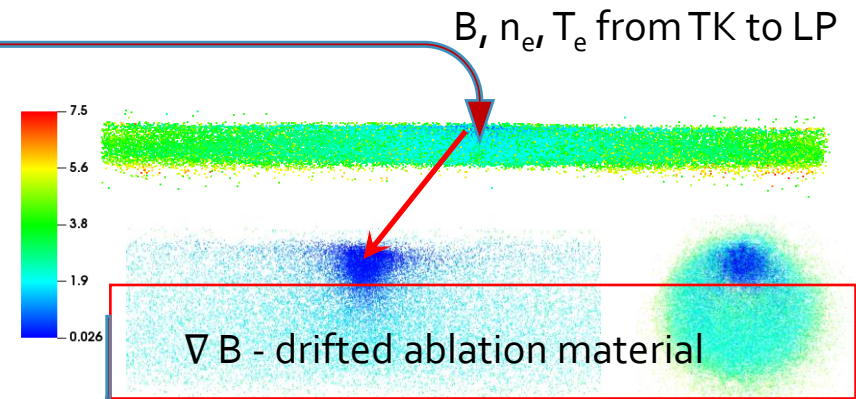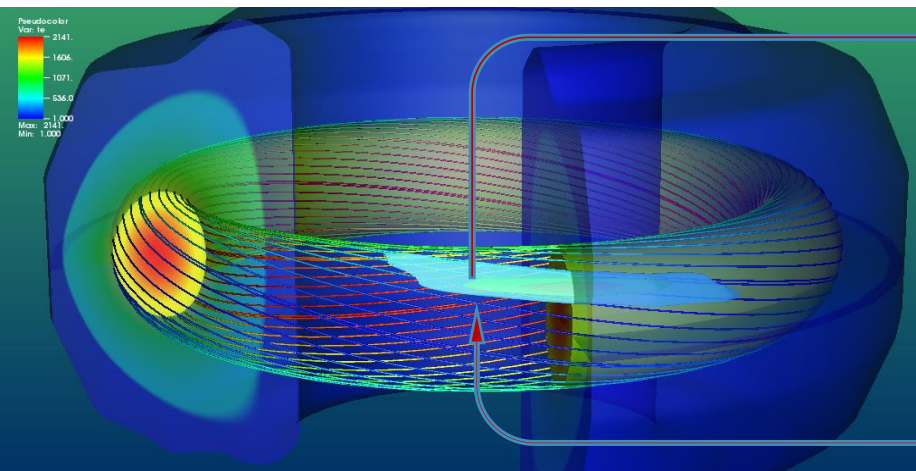
Mass flow, thermodynamic data, and energy sinks from LP to TK

- LP code evolves self-consistently the entire ablation cloud that provides pellet shielding
- Ablated material that drifted beyond the main ablation cloud is transferred to the tokamak code, (together with thermodynamic data and energy sinks)
- LP code obtains the magnetic field and electron density and temperature from the tokamak code
- The first step of data transfer from the LP code to NIMROD and M3D-C^1 has been accomplished

R. Samulyak, C. Kim, B. Lyons, N. Ferraro   29

Center for Tokamak Transient Simulations
Outline

1. Code Descriptions

2. Forces due to Vertical Displacement Events

3. Disruption Mitigation via Impurity Injections
   3.1 Stand Alone
   3.2 via code coupling

4. **Runaway Electrons interacting with MHD**

5. High-Performance Computing

Integrated modeling of Runaway Electrons (RE) with MHD

- New fluid runaway electron modules for both M3D-C^1 and NIMROD are now being evaluated.

  - RE generation mechanisms (hot-tail, tritium-decay, avalanche), which are important in ITER, are included.

  - The new modules will be used in VDE simulations to determine the effect of RE current on MHD & vessel forces.

- A collaboration between PPPL, GA, and ORNL is initialized to couple both M3D-C^1 and NIMROD with KORC to model runaway electron diffusion and its back reaction to MHD instabilities

  KORC: Highly scalable PIC RE code using GPUs (ORNL)

Perturbed current of (1,1) mode
From M3D-C^1 without RE current

Perturbed current of (1,1) mode with RE current

C. Liu, C. Zhao

Center for Tokamak Transient Simulations
Outline

Must Address Communication to Improve Scaling Performance

- SuperLU Preconditioners are essential for the solvers in M3D-C[1] and NIMROD

- Solver performance is dominated by MPI communications in the triangular solve

- Performance improvements in SpTRSV improves application performance and scalability

- COMPARED SIX MATRICES
  - 1 from FES code M3D-C[1] A30
  - 5 from SuiteSparse Matrix Collection

- COMMUNICATION ~70% - 90% FOR ALL LARGE SPARSE MATRIX SOLVES

■ Others ■ Communication
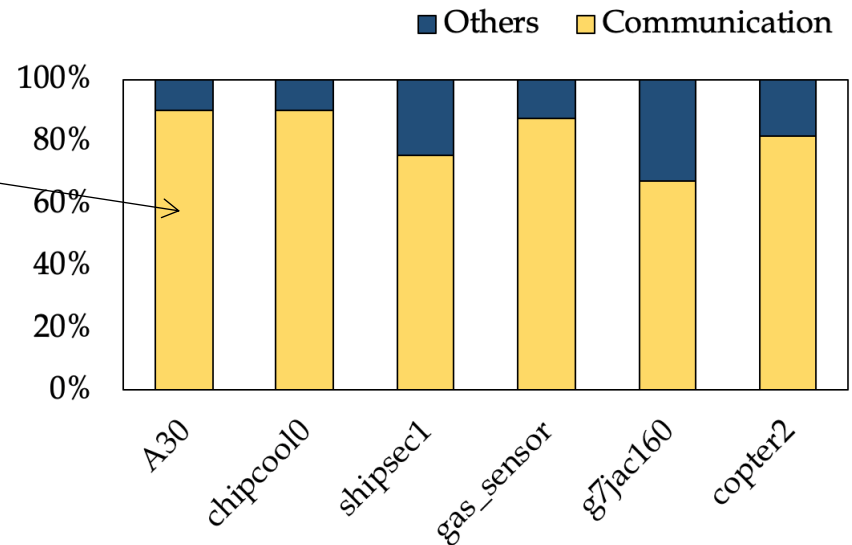
Solve time break down
on NERSC's Cori/KNL using 1024 processes

SpTRSV: SuperLU_dist triangular solve

N. Ding, S. Williams, S. Li, Y. Liu

Performance model for Sparse Triangular Solvers

- LBL built a critical path analysis tool to determine the critical path with consideration of process decomposition
    - Circles can represent:
        - a DGEMV or TRSMV in SpTRSV
        - a kernel in the application
    - Edges can represent:
        - data dependencies
        - execution flow

- LBL modeled mat-vecs and communication in SpTRSV using the critical path analysis tool
    - Empirical observations of performance fit within the model's performance bounds

Critical path visualization

DGEMV & TRSMV are matrix-vec operations
SpTRSV: SuperLU_dist triangular solve

N. Ding, S. Williams, S. Li, Y. Liu

34
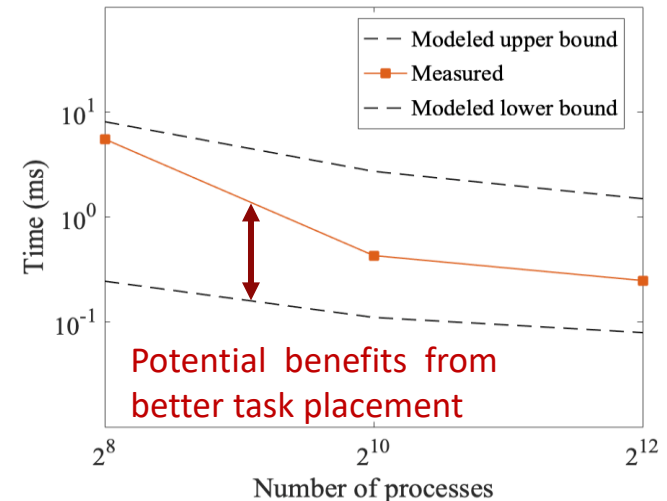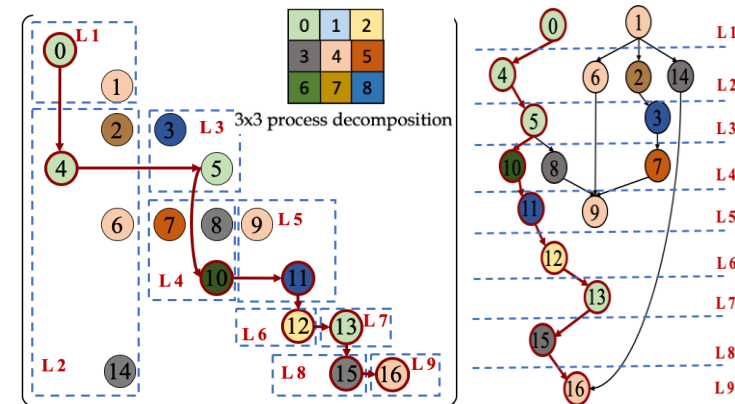
Implementing One-Sided Communication:

- Remote direct memory access (RDMA) is a process to directly access memory on remote processes without involvement of the activities at the remote side.

- Light-weight asynchronous primitives provides a pathway to efficient DAG execution and accelerator-based exascale solvers

- Shown below: fompi one-sided communication greatly improves bandwidth over MPI two-sided
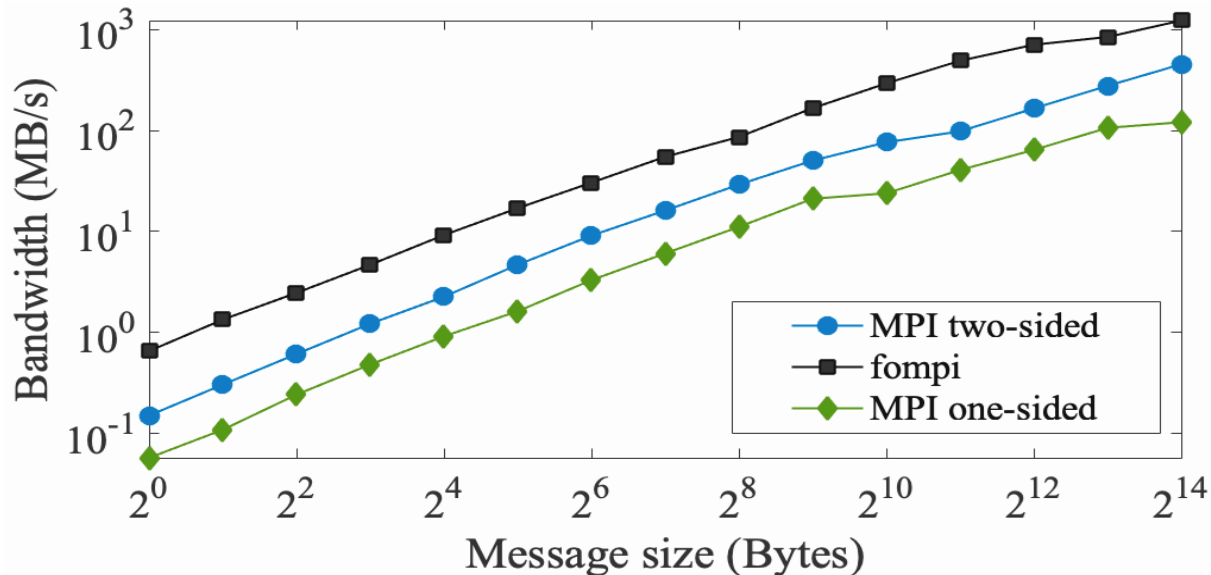
DAG: Directed Acyclic Graph

One-Sided Communication implemented for Sparse Triangular Solvers

- LBL created a one-sided MPI version of SpTRSV on Cray system

- Attained a 2.2x speedup for M3D-C^1 matrix at 4096 processes on Cori(NERSC) over the existing two-sided in SuperLU_DIST

SpTRSV: SuperLU_dist triangular solve

N. Ding, S. Williams, S. Li, Y. Liu
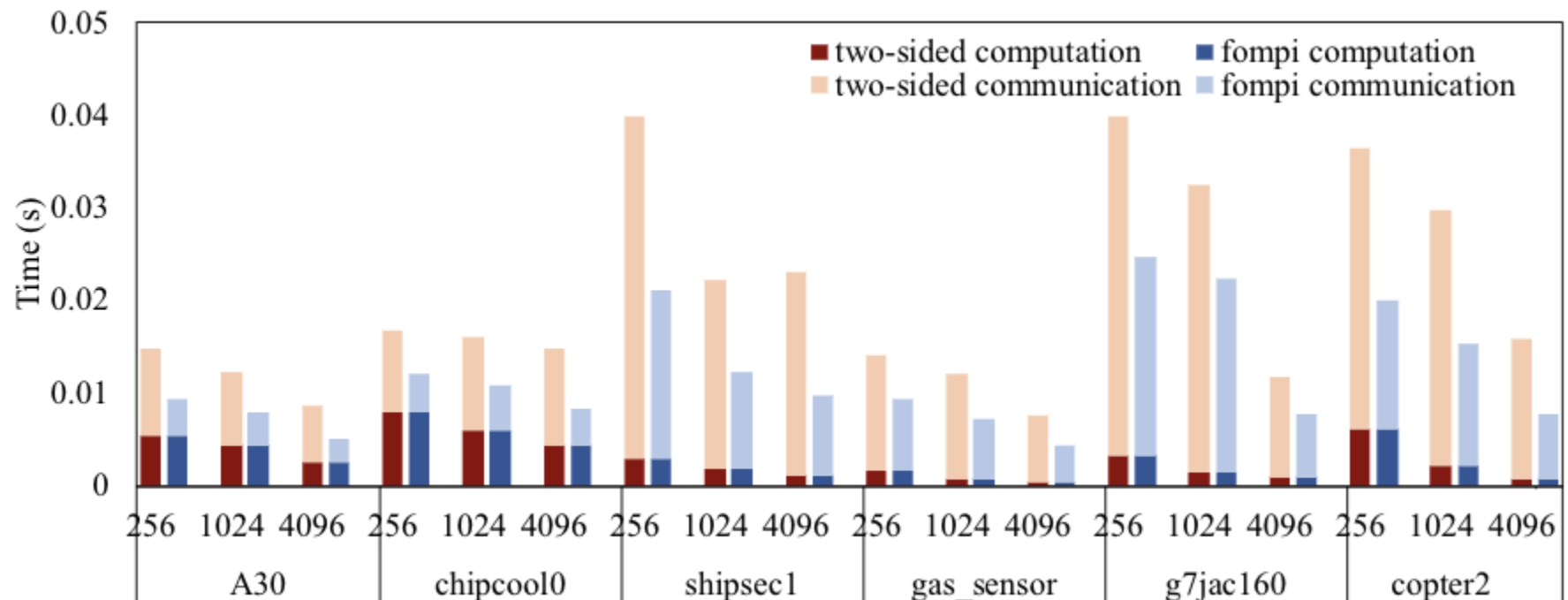
Communication-avoiding 3D sparse LU factorization in SuperLU_dist

- **Algorithm innovation**: 3D grid of MPI processes, Z-dimension has some data replication, but results in reduced communication and increased parallelism
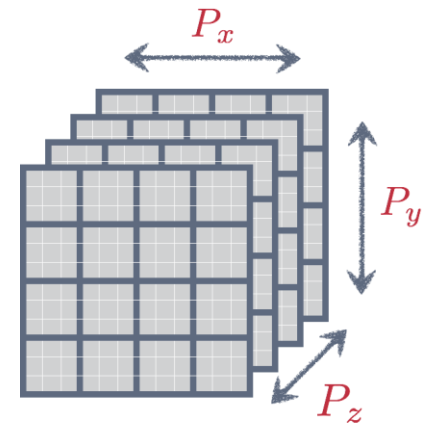
- Shown in graph is improvement in M3D-C[1] velocity matrix for 32, 128, 512 MPI processes: (1.3x, 1.8x, 5x)

M3D-C1: dimension 120K
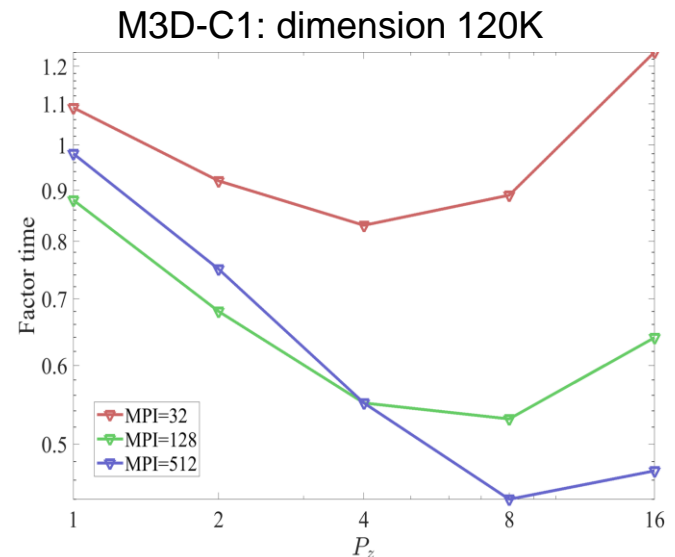
$$\mathbf{V} = R^2\nabla U \times \nabla\varphi + \omega R^2\nabla\varphi + R^{-2}\nabla_\perp\chi$$

Velocity Matrix Restructuring for Improved Preconditioning

- M3D-C[1] uses a physics-based Helmholtz-like decomposition of the velocity field:

$$\mathbf{V} = R^2\nabla \textcolor{red}{U} \times \nabla\varphi + \textcolor{red}{\omega} R^2\nabla\varphi + R^{-2}\nabla_\perp\textcolor{red}{\chi}$$

- The old ordering mixed these 3, physically different velocity variables in the same vector

- New ordering allows us to separate these, facilitating a more efficient pre-conditioning strategy.

(R, φ, Z) coordinates

Because each toroidal plane couples only to adjacent toroidal planes, the full velocity matrix is of block-tridiagonal form.   Corner elements due to periodicity.
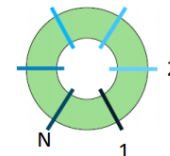
$$
\begin{bmatrix}
\mathbf{B}_1 & \mathbf{C}_1 & & & \mathbf{A}_1 \\
\mathbf{A}_2 & \mathbf{B}_2 & \mathbf{C}_2 & & \\
& \ddots & \ddots & \ddots & \\
\mathbf{C}_N & & \mathbf{A}_N & \mathbf{B}_N
\end{bmatrix}
\cdot
\begin{bmatrix}
\mathbf{X}_1 \\
\mathbf{X}_2 \\
\vdots \\
\mathbf{X}_N
\end{bmatrix}
=
\begin{bmatrix}
\mathbf{Y}_1 \\
\mathbf{Y}_2 \\
\vdots \\
\mathbf{Y}_N
\end{bmatrix}
$$

$\mathbf{X}_j$ contains all the velocity variables on plane j
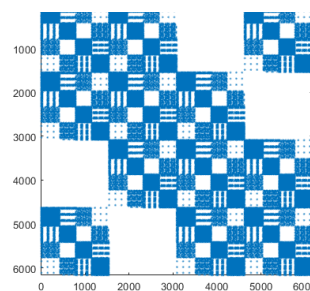
per-process   per-plane   global
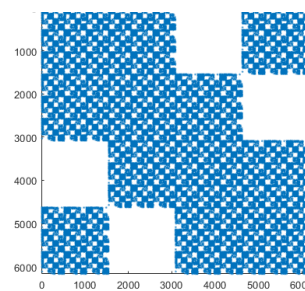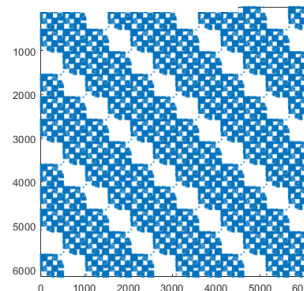
W. Tobin, M. Shephard, E. Seol

Adjacency – based reordering has potential to improve performance
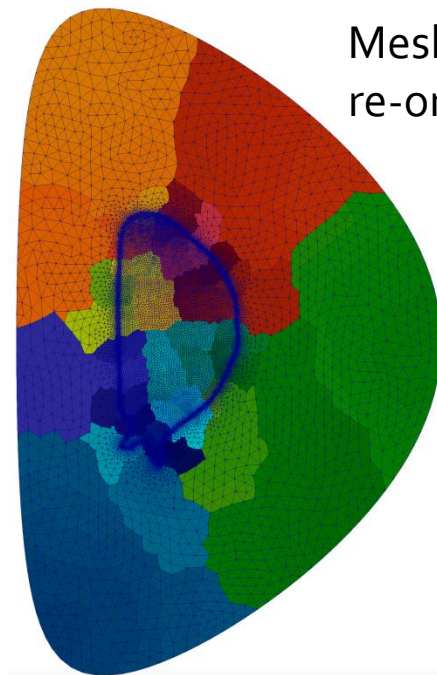
Mesh without re-ordering
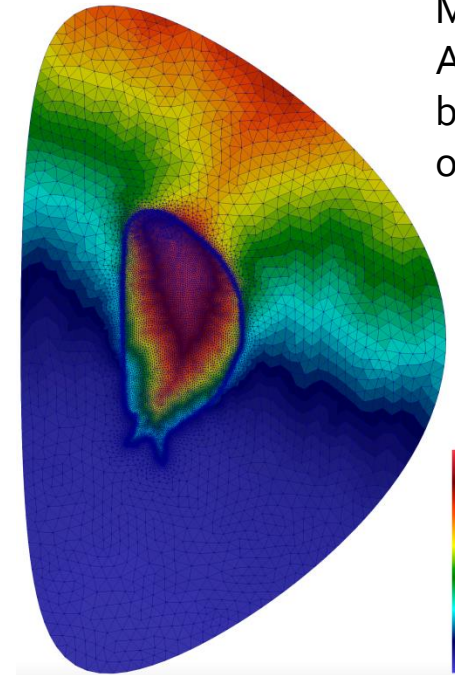
Mesh with Adjacency-based re-ordering

- Colors correspond to mesh numbering: blue → red
- Re-ordering can improve cache misses and Particle-in-Cell performance
- Now being evaluated for M3D-C^1 and NIMROD

E. Seol, M. Shephard, W. Tobin

Center for Tokamak Transient Simulations:
THANK YOU

1. Code Descriptions

2. Forces due to Vertical Displacement Events

3. Disruption Mitigation via Impurity Injections
   3.1 Stand Alone
   3.2 via code coupling

4. Runaway Electrons interacting with MHD

5. High-Performance Computing

Extra slides